HHS Public Access

Author manuscript

J Nat Prod. Author manuscript; available in PMC 2016 August 28.

Published in final edited form as:

J Nat Prod. 2015 August 28; 78(8): 1990–2000. doi:10.1021/acs.jnatprod.5b00288.

Silymarin Suppresses Cellular Inflammation By Inducing Reparative Stress Signaling

Erica S. Lovelace[†], **Jessica Wagoner**[†], **James MacDonald**[‡], **Theo Bammler**[‡], **Jacob Bruckner**[†], **Jessica Brownell**[§], **Richard Beyer**[‡], **Erika M. Zink**[⊥], **Young-Mo Kim**[⊥], **Jennifer E. Kyle**[⊥], **Bobbie-Jo Webb-Robertson**[⊥], **Katrina M. Waters**[⊥], **Thomas O. Metz**[⊥], **Federico Farin**[‡], **Nicholas H. Oberlies**[▽], and **Stephen J. Polyak**[†,‖,○,*]

[†]Department of Laboratory Medicine, University of Washington, Seattle, WA, United States, 98104

[‖]Department of Global Health, University of Washington, Seattle, WA, United States, 98104

[○]Department of Microbiology, University of Washington, Seattle, WA, United States, 98104Center for Ecogenetics and Environmental Health, University of Washington, Seattle, United States, 98105

[‡]Department of Environmental and Occupational Health Sciences, University of Washington, Seattle, United States, 98105

[§]Malaria Program, Seattle Biomed, Seattle, United States, 98109

[⊥]Biological Sciences Division Pacific Northwest National Laboratory, Richland, WA, United States

[▽]Department of Chemistry and Biochemistry, University of North Carolina at Greensboro, NC, United States

Abstract

Silymarin, a characterized extract of the seeds of milk thistle (*Silybum marianum*), suppresses cellular inflammation. To define how this occurs, transcriptional profiling, metabolomics, and signaling studies were performed in human liver and T cell lines. Cellular stress and metabolic pathways were modulated within 4 h of silymarin treatment: activation of Activating Transcription Factor 4 (ATF-4) and adenosine monophosphate protein kinase (AMPK) and inhibition of mammalian target of rapamycin (mTOR) signaling, the latter being associated with induction of DNA-damage-inducible transcript 4 (DDIT4). Metabolomics analyses revealed silymarin suppression of glycolytic, tricarboxylic acid (TCA) cycle, and amino acid metabolism. Anti-inflammatory effects arose with prolonged (i.e. 24 h) silymarin exposure, with suppression of multiple pro-inflammatory mRNAs and signaling pathways including nuclear factor kappa B (NF-

[*]**Corresponding Author:** (S.J. Polyak). Tel: 1-206-897-5224. Fax: 1-206-897-4312. polyak@uw.edu.

Supporting Information. Primer-probe sets for RT-PCR validation of microarray data and antibodies used in Western blotting are in Tables S1 and S2, respectively. Figures S1–S9 provide microarray heat map, microarray RT-PCR validation, protein validation, supporting IPA pinwheels, metabolomics heat map, AMPK knockout validation, and IPA legend. This material is available free of charge via the Internet at http://pubs.acs.org.

Author Contributions

The manuscript was written through contributions of all authors. All authors have given approval to the final version of the manuscript.

κB) and forkhead box O (FOXO). Studies with murine knock out cells revealed that silymarin inhibition of both mTOR and NF-κB was partially AMPK dependent, while silymarin inhibition of mTOR required DDIT4. Other natural products induced similar stress responses, which correlated with their ability to suppress inflammation. Thus, natural products activate stress and repair responses that culminate in an anti-inflammatory cellular phenotype. Natural products like silymarin may be useful as tools to define how metabolic, stress, and repair pathways regulate cellular inflammation.

Natural products are used to prevent and treat a plethora of chronic, debilitating, and inflammatory diseases. Over one-third of adults in the US reported self-medicating with complementary and alternative medicines (CAM).[1] Defining precise mechanisms of action is a critical barrier to the optimal application of botanicals as CAMs and as pharmaceuticals. Natural products, like the compounds contained in silymarin (a.k.a. milk thistle extract; from the plant *Silybum marianum* [L.] Gaertn. [Asteraceae]), protect cells by various antioxidant, anti-inflammatory, antiviral, immunomodulatory, proliferative, and metabolic effects,[2,3] resulting in diverse protective phenotypes, both *in vitro* and *in vivo*. For example, silymarin and silymarin-derived flavonolignans inhibit *in vitro* hepatitis C virus (HCV) infection of human liver cell cultures, HCV-induced oxidative stress, NF-κB pro-inflammatory signaling, and T cell activation and inflammatory cytokine production.[4] Although there is a clear precedence for silymarin and silbinin, the major component of silymarin, having anti-cancer,[5] and cytoprotective effects,[6] an integrated view of the cellular responses and pathways behind these phenotypes has not been established. While the anti-cancer activities of silymarin arise via induction of cell death, it is not clear how non-toxic doses of silymarin confer cellular protection in the form of reduced cellular inflammation.

Environmental cues such as energy restriction, oxygen depletion, and viral infection activate stress responses in a cell. By triggering stress pathways, the cell initiates responses that result in either adaptation (through reparative responses) or cell death (via apoptosis, necrosis, or pyroptosis). Regardless of the final cellular fate, there exists common cellular responses to stress such as early metabolic and cell cycle changes,[7] damage repair processes,[8] and the initiation of protective mechanisms, such as induction of antioxidant response genes.[9]

Cell responses to stress are initiated often with cross talk between key metabolic signaling kinases and transcription factors. For example, the mammalian target of rapamycin (mTOR), involved in approximately 80% of all cancers,[10] is a major hub for several metabolic inputs and cues. By sensing energy status, mTOR affords switching between anabolic (in a nutrient-rich environment) and catabolic (during stress) cellular processes. Thus, when nutrients are abundant, mTOR kinase activity leads to the phosphorylation of several downstream targets including eukaryotic translation initiation factor 4E-binding protein (4EBP-1) and S6 kinase (S6K), which promotes cellular anabolism. Conversely, mTOR signaling is inhibited during amino acid depletion.[11,12]

mTOR receives input from multiple stress-sensing pathways. For example, when the 5′ adenosine monophosphate-activated protein kinase (AMPK) pathway is activated and phosphorylated by energy stress (i.e. decreased cellular ATP/ADP ratios), it inhibits the

mTOR pathway.[13] Moreover, the expression of DNA damage-inducible transcript 4 (DDIT; also known as REDD1), a major negative regulator of mTOR activity, is induced during stress.[14,15] During endoplasmic reticulum (ER) stress, the translational control factor eukaryotic initiation factor 2-alpha (eIF2α) becomes phosphorylated on a conserved serine residue, leading to translational repression of most cellular mRNAs with the exception of a few key stress-response proteins, such as ATF4. Moreover, the mTOR pathway also converges on the transcription factor FOXO3a, which plays pivotal roles in determining cellular fates (adaptation vs. death) to environmental stress by altering metabolism, initiating immune responses, and initiating apoptosis.[16]

This study presents the first transcriptional and metabolomics profiling study of silymarin-treated human liver-derived cells with protein and signaling validation in both human liver and T cell cultures. It is shown that non-toxic doses of silymarin initially induce ER and energy stress responses, and that instead of dying, the cell responds to these stresses with adaptive and reparative responses. In this environment, cells adapt to the non-toxic stress by establishing a cellular milieu that is anti-inflammatory. Moreover, metabolic pathways, like AMPK, that are modulated by silymarin, are involved in suppression of mTOR and inflammatory (i.e. NF-κB) signaling. Finally, other natural products induced similar stress responses, which correlate with their ability to suppress inflammation. Using natural products as tools to define how cellular stress links to inflammatory status may reveal opportunities for selective reprogramming of cellular metabolism in order to alter immune and inflammatory responses in both health and disease.

RESULTS AND DISCUSSION

This workflow of this study started with a whole genome microarray study of silymarin versus DMSO solvent control treated human hepatoma Huh7.5.1 cells for four, eight, and 24 h. These time points were chosen in order to capture the earliest transcriptional changes in a cell following exposure to silymarin. Preliminary whole genome microarray studies were also performed following one h and four h of silymarin exposure. Unsupervised hierarchical clustering of differentially expressed transcripts revealed that silymarin–specific clustering only occurred with the 4h treatment (data not shown). Thus, four h was chosen as the earliest time point. Gene expression data were then analyzed by various bioinformatics software to identify key genes and pathways modulated by silymarin. Microarray results were then validated by independent gene expression assays (quantitative reverse transcriptase polymerase chain reaction (qRT-PCR)) and protein expression by Western blot. Gene expression analysis suggested silymarin was altering cellular metabolism. As such, a metabolomics study was also performed. Pathways modulated by silymarin were validated by signal transduction studies in Huh7.5.1 cells and Jurkat T cells. Huh7.5.1 human hepatoma cells and Jurkat T cells were chosen for this study because we have previously shown that silymarin inhibits inflammatory signaling via NF-κB in these cell types[4,17], and they are also relevant model systems to study HCV and HIV infection-associated inflammation.

In human hepatoma Huh7.5.1 cells, a non-toxic dose of 80 μM silymarin or DMSO for four h resulted in the significant differential expression of 82 mRNAs, with 67 mRNAs

significantly induced and 15 mRNAs significantly inhibited. The number of genes modulated by silymarin treatment grew over time, with 98 and 58 genes significantly induced and 165 and 188 genes significantly repressed at the eight and 24 h time points, respectively.

There were two major patterns of transcriptional regulation induced by silymarin treatment. As shown in the heat map in Figure S1, Supporting Information, 443 genes were differentially expressed between the DMSO and silymarin treatments at four, eight, and 24 h. The first pattern (highlighted in the right third of the heat map) was a significant induction of mRNAs by silymarin treatment at four h that remained elevated at eight and 24 h. The second pattern of mRNA expression (highlighted in the left-most section of the heat map) was unchanged at four h, decreased slightly by eight h and was strongly suppressed by the 24-h time point. Thus, the cellular response to silymarin treatment was biphasic: an initial and sustained induction of gene expression, followed by progressive suppression of mRNAs with prolonged silymarin treatment.

Eighteen significantly up-regulated and down-regulated genes were further validated by qRT-PCR (Figure S2A, Supporting Information). Genes were selected primarily if they showed strong regulation by silymarin. Some genes were secondarily selected based on biological relevance to the anti-inflammatory actions of silymarin. There was strong correlation between array and qRT-PCR results of the gene expression patterns for all 18 genes compared across all time points (Figure S2B, Supporting Information). As shown in Figure S3A, Supporting Information, *DDIT4* (*REDD1*) mRNA was one of the most highly induced transcripts observed with silymarin treatment. By qRT-PCR, *DDIT4* mRNA was significantly induced at four, eight, and 24-h post-silymarin treatment. Silymarin treatment also induced DDIT4 protein in Huh7.5.1 cells (Figure S3B, Supporting Information). In contrast, *CXCL10*, a highly pro-inflammatory gene, was the most down-regulated mRNA post-silymarin treatment. *CXCL10* mRNA was most suppressed at the 24-h time point, exemplary of the progressive temporal decline in gene expression due to silymarin treatment (Figure S3C, Supporting Information). Furthermore, silymarin dose-dependently reduced *CXCL10* mRNA and CXCL10 protein expression in Jurkat cells co-stimulated by IFNγ and TNFα (Figure S3D, Supporting Information), demonstrating that silymarin treatment inhibited induction of the chemokine CXCL10 in two distinct cell types.

Silymarin Induces Endoplasmic Reticulum Stress

The first focus was to determine the cell signaling events behind the initial and sustained induction of gene expression. Bioinformatics analyses using IPA software (Figure S9, Supporting Information) revealed that genes associated with endoplasmic reticulum (ER) stress were significantly induced at four and eight h post-silymarin treatment, with many ER stress genes remaining significantly up-regulated at the 24-h time point. IPA predicted that ATF4, a key transcription factor involved in ER stress, was directly involved in the rapid induction of gene expression following silymarin treatment. Twelve ATF4-regulated mRNAs were induced at four h (Figure 1A), and most ATF4-regulated genes remained induced at eight and 24 h post-silymarin treatment in Huh7.5.1 cells (Figure S4A and B, respectively). ATF4 protein induction was verified by treating Huh7.5.1 and Jurkat cells

with silymarin. Thapsigargin, a natural product, was included as a positive control for induction of ER stress[18]. Indeed, eIF-2α phosphorylation (Ser51) and ATF4 protein expression were clearly induced in a dose-dependent manner after one h silymarin treatment of Huh7.5.1 cells (Figure 1B). In Jurkat cells, both eIF-2α phosphorylation and ATF4 protein expression were similarly increased with silymarin treatment in a dose-dependent manner as early as 30 minutes post-silymarin treatment (Figure 1C).

Silymarin Activates AMPK and Inhibits mTOR

The activation of AMPK is a major sensor of cellular energy status that connects nutrient sensing and ER stress pathways.[19] As shown in Figure 2, silymarin caused dose-dependent activation of AMPK (measured as increased phosphorylation at position Thr172) in Huh7.5.1 (Figure 2A) and Jurkat cells (Figure 2B). AMPK activation was observed as early as one h after silymarin treatment in both Huh7.5.1 and Jurkat cells.

Since DDIT4 is a known negative regulator of mTOR,[15] and *DDIT4* mRNA and DDIT4 protein were strongly induced as early as four h post-silymarin treatment (Figure S4A, Supporting Information and Figure 1B, respectively), the mTOR pathway was tested for inhibition by silymarin. Silymarin inhibited serum-induced phosphorylation and activation of mTOR (Ser2448), 4EBP-1 (Thr37/46), and p70S6 Kinase (referred to as S6K) (Thr389) in Huh7.5.1 (Figure 2C). Moreover, silymarin treatment (80 μM) modestly inhibited mTOR signaling in Jurkat cells cultured in complete medium (Figure 2D).

Silymarin Modulates Cellular Metabolism

To better understand the mechanism by which silymarin treatment induced stress signaling in cells, metabolomics analyses were performed on a derivative of Huh7 cells that express Toll-like Receptor 3 (TLR3).[20] These cells were chosen because they express functional retinoic acid inducible gene 1 (RIG-I) and TLR3, the two pathogen recognition receptors for HCV[21,22]. Huh7-TLR3 cells were treated with silymarin (80 μM) for four, eight, and 24 h. Silymarin treatment caused statistically significant ($p < 0.05$) decreases (up to four-fold) in abundances at one or more time points for nearly half of 95 measured metabolites, including glycolytic and TCA cycle intermediates, amino acids, and sugars (Table 1, Figure S5, Supporting Information). However, no statistical differences were observed in the abundances of nucleobases, nucleosides, and related metabolites, or in free fatty acids, suggesting that cell metabolism was not uniformly affected (Table 1). Interestingly, pantothenic acid (vitamin B5) was the only metabolite that showed statistically significant ($p < 0.001$) increases (over two-fold) in abundance at all time points.

Silymarin Inhibits Inflammatory Signaling

The next focus was to determine the signaling events behind the second component of the biphasic cellular response to silymarin treatment: the progressive, temporal suppression of gene expression. IPA predicted that silymarin treatment inhibited the inflammatory response (Figure 3A). For example, IPA revealed NF-κB as a key upstream regulator involved in silymarin treatment signaling. Widespread, silymarin-induced suppression of NF-κB-dependent gene expression in Huh7.5.1 cells is shown in Figure 3B, where silymarin treatment resulted in the significant modulation of 32 mRNAs, with many having pro-

inflammatory functions. Moreover, IPA predicted cross talk between the ATF4, FOXO3 (see below), and NF-κB pathways, suggesting that stress pathways communicate to pro-inflammatory pathways (Figure 3C).

By 24 h post-silymarin treatment, silymarin–induced suppression of inflammation extended to inhibition of multiple CC and CXC pro-inflammatory cytokine and chemokine mRNAs in Huh7.5.1 cells. For example, silymarin treatment resulted in the significant down-regulation of *CCL20*, *CXCL1*, *CXCL10*, *CXCL5*, and *CXCL6* mRNAs. Moreover, IPA predicted the inhibition of several cytokine and chemokine upstream regulators, receptors, and complexes including interleukin-6 (IL-6), interleukin-17A (IL-17A), and transforming growth factor beta (TGFβ) (Figure S6A–C, Supporting Information). Silymarin treatment also caused significant suppression of many non-chemokine, non-cytokine mRNAs that are involved in the inflammatory response, such as nucleotide-binding oligomerization domain containing 2 (NOD2), a protein expressed in peripheral blood leukocytes, and interleukin-1 receptor-associated kinase 4 (IRAK4), a kinase that activates NF-κB in both the Toll-like receptor and T-cell receptor signaling pathways, respectively (Figure S6D and S7E, Supporting Information). Moreover, IPA predicted the silymarin-inhibition of many upstream regulators involved in the immune regulation known to be involved in the lipopolysaccharide (LPS) response (Figure S6F, Supporting Information).

IPA also predicted that silymarin treatment modulated the FOXO3 transcription factor. Specifically, FOXO3- regulated genes became progressively inhibited at eight and 24 h post-silymarin treatment (Figure S7A, Supporting Information). Since FOXO3 activity is inhibited by phosphorylation,[23] the effect of silymarin treatment on FOXO3 phosphorylation (Ser256) was examined. Silymarin treatment resulted in increased phosphorylation of FOXO3 (Figure S7B, Supporting Information). Thus, silymarin treatment suppressed FOXO3 activity and FOXO3- dependent gene expression in liver and T cell cultures.

Collectively, the data indicate that prolonged exposure of cells to silymarin results in global suppression of multiple, interconnected inflammatory signaling pathways.

Silymarin Induction of Stress Signaling is Linked to Suppression of Inflammation

Next explored were the connections between the induction of stress responses (i.e. suppression of mTOR, activation of AMPK) and the inhibition of inflammatory signaling (i.e. NF-κB) that occurred with silymarin treatment. Firstly, since silymarin induced DDIT4 protein, and mTOR is known to be inhibited by DDIT4,[24] silymarin's ability to suppress mTOR in DDIT4 knockout mouse (KO) embryo fibroblasts (MEFs)[25] was evaluated. In wild type (WT) MEFs, cobalt chloride, known to up-regulate DDIT4,[26] induced DDIT4 protein, which was associated with inhibition of phosphorylation of the mTOR target S6K. Cobalt chloride also increased the mobility of 4EBP1 (i.e. the protein migrated faster in the polyacrylamide gel; Figure 4A). Since phosphorylated 4EBP1 migrates slower and produces a gel shift in polyacrylamide gels,[27] the increased/faster mobility of 4EBP1 with cobalt chloride treatment indicates a reduction in 4EBP1 phosphorylation. As expected, cobalt chloride did not inhibit S6K and 4EBP1 phosphorylation in DDIT4 KO MEFs. In WT MEFs, silymarin modestly induced DDIT4 protein and also reduced S6K phosphorylation as

well as increased the mobility of 4EBP1 (i.e decreased phosphorylation). Similarly to cobalt chloride, in DDIT4 KO MEFs, silymarin treatment no longer induced DDIT4 protein nor reduced S6K phosphorylation nor increased 4EBP1 mobility (Figure 4A). The data suggest that silymarin inhibits mTOR signaling via induction of DDIT4.

Secondly, to investigate silymarin inhibition of mTOR via the AMPK signaling axis, MEFs containing WT or a double KO of AMPKα1 and α2 subunits[28] were used. The phenotypes of WT and AMPK KO cells was confirmed by measuring levels of phosphorylated AMPK and Acetyl-CoA Carboxylase (ACC), an AMPK target, upon silymarin exposure (Figure S8, Supporting Information). In WT MEFs, both silymarin and rapamycin treatment, a mTOR inhibitor, reduced phosphorylation of mTOR and S6K, as well as increased the mobility of 4EBP1 (Figure 4B). In contrast, in AMPK KO MEFs, silymarin treatment no longer inhibited mTOR phosphorylation or increased the mobility of 4EBP1, although higher doses of silymarin still partly inhibited S6K phosphorylation (Figure 4B). Rapamycin suppression of mTOR was unaffected by deletion of AMPK, as expected for a direct mTOR inhibitor. The data suggest that silymarin inhibits mTOR via the AMPK pathway.

Since AMPK sensing of cellular energy status influences NF-κB activity,[29] it was next determined whether silymarin inhibition of NF-κB was dependent on AMPK. Silymarin treatment caused significant, dose-dependent inhibition of TNF-α induced NF-κB-dependent transcription in WT MEFs ($p<0.02$; Figure 4C). In contrast, in the AMPK KO MEFs, silymarin suppression of NF-κB-dependent transcription was significantly attenuated ($p<0.02$). Collectively, the data suggest that silymarin suppression of mTOR signaling is in part dependent on both AMPK and DDIT4, while silymarin suppression of NF-κB is in part AMPK dependent. Therefore, silymarin-induced stresses are relayed via metabolism-sensing signaling pathways to suppress cellular inflammation.

The First Phase: Induction of Stress Responses

In this report, it was shown that the biphasic response to silymarin treatment was initiated with several cellular stress responses: activation of AMPK signaling, induction of *DDIT4* mRNA and protein expression, inhibition of mTOR signaling, and induction of ER stress. Our data are consistent with previous studies showing that silibinin inihbits the mTOR pathway upstream of tuberous sclerosis 2 (TSC2) and downstream of phosphatase and tensin homolog (PTEN).[30] This is the first demonstration that silymarin may control mTOR via DDIT4. In addition, it is shown for the first time that silymarin treatment also activates AMPK, further supporting the role of silymarin treatment in inducing ER stress pathways. Herein, it is also shown that silymarin treatment resulted in a reduction of cellular metabolism, which has been shown to lead to AMPK activation.[31]

Transition of the Biphasic Response from Stress and Repair to Blockade of Inflammation

This study reveals that AMPK is a key mediator involved in transducing the signal from silymarin-induced stress to anti-inflammatory effects. Indeed, numerous studies have shown the correlation between AMPK, mTOR, and their interplay with NF-κB, FOXO, and chemokine signaling, as well as their links to metabolism in chronic inflammation and disease.[32–36] It was also shown that silymarin inhibited FOXO3: a key conduit between cell

metabolism, growth, and inflammation and immunity.[37] Silymarin also inhibited the mTOR pathway in Jurkat cells, consistent with previous studies in activated T cells.[38] Silymarin and compounds within the extract, particularly silibinin, inhibit NF-κB, a pivotal transcription factor involved in inducing the expression of many pro-inflammatory genes.[4,39–41] Furthermore, the use of WT and KO MEFs revealed that silymarin activation of AMPK signaling was partially responsible for silymarin inhibition of both mTOR and NF-κB signaling. AMPK-regulated sensing has also been shown to directly regulate inflammation: as cellular energy levels drop, AMPK becomes activated, which inhibits energy-consuming (anabolic) pathways, including cellular inflammation.[24,29,42,43] Thus, silymarin treatment resulted in the regulation of cellular stress responses to control inflammation and immunity.[2]

The Second Phase: Inhibition of Inflammation

It was also demonstrated that the initial stress response of silymarin treatment transitions over time into the anti-inflammatory half of a biphasic response, and this is associated with suppression of many inflammatory genes such as CXCL10, in both liver and T cell cultures. These findings may be of relevance in inflammatory diseases since enhanced tissue expression of CXCL10 has been associated with many autoimmune diseases.[44] Furthermore, CXCL10 over-expression has been shown to correlate with disease progression in several chronic infectious diseases such as HCV[20,45,46] and human immunodeficiency virus-1 (HIV-1) infections.[47] Thus, natural products like silymarin may be useful tools to dissect how stress signaling regulates pro-inflammatory signaling and cytokine production.

Natural Products that Suppress Inflammation also Induce Stress Responses

Chemically distinct, plant-derived natural products display anti-inflammatory, anti-proliferative, and anti-oxidant responses that are similar to those induced by silymarin treatment.[10,48–52] For example, curcumin and epigallocatechin gallate (EGCG) induce anti-inflammatory effects, modulate mTOR/PI3K signaling, and activate antioxidant pathways.[49,53,54] In addition, many natural products such as resveratrol, EGCG, capsaicin, and curcumin affect AMPK pathways.[55] Other polyphenols also modulate inflammatory pathways[56], and EGCG modulates FOXO3.[57] IPA revealed that many mRNAs that were significantly regulated by silymarin overlapped with many of the known gene expression changes induced EGCG and curcumin (Figure 5A). For example, the significant suppression of inflammatory mRNAs with silymarin treatment overlapped with the anti-inflammatory transcriptional changes reported for EGCG and curcumin (e.g. suppression of *CXCL8*, *CXCL10*, and *NFKB1A* mRNAs). Given that silymarin induction of stress is at least partly involved in suppression of inflammation (Figure 4C), it was determined whether EGCG and curcumin also induce similar stress responses. In Figure 5B, EGCG and curcumin treatment in Huh7.5.1 cells resulted in an upregulation of ATF4 (a marker of ER stress), DDIT4 (a marker for mTOR inhibition), and phosphorylated AMPK (a marker of reduced cellular metabolism) protein expression. Thus, chemically distinct natural products appear to induce similar cellular stress responses, which correlates with their ability to suppress inflammation.

The data presented in this study suggest that non-toxic doses of silymarin induce cytoprotection via a biphasic process that initially involves suppression of cellular metabolism and activation of stress pathways, followed temporally by progressive down-regulation of inflammatory signaling. The response to silymarin treatment observed in this study was not limited to liver cells, as silymarin treatment of T cells caused similar responses. The biphasic transcriptional response to silymarin treatment is reminiscent of temporal hormesis,[58] the process by which initial administration of a chemical exerts cellular stress, followed by beneficial and protective effects with prolonged exposure.[58] Similar to the findings in the present study, other natural products have been shown to induce biphasic dose responses.[59,60]

Further research into how natural products alter cellular metabolism and initiate stress signaling, to favor repair and survival over cell death, and how these pathways connect to inflammatory signaling, may reveal novel avenues for exploiting the health promoting effects of natural products via CAM approaches, as well as for the development of new chemotherapeutics that quell pathogenic inflammation.

EXPERIMENTAL SECTION

Cells and Reagents

Huh7.5.1 and Huh7-TLR3 cells are derived from Huh7 cells[61,62]. They were cultured as described.[63] Jurkat T cells were cultured as described.[17] WT and DDIT4 knock out murine embryo fibroblasts (MEF) were obtained from Leif Ellisen, while WT and AMPK knock out MEFs were obtained from Benoit Viollet. Powdered extract (Product No. 345066, Lot No. 286061) of the seeds (achenes) of *Silybum marianum* [L.] Gaertn. was obtained from Euromed, S.A. (Barcelona, Spain), which is a part of the Madaus Group (Cologne, Germany). To eliminate stability concerns with freeze-thawing solutions of silymarin and the hygroscopic nature of DMSO, single use aliquots of silymarin were prepared as follows. The extract was reconstituted to a concentration of 10 mM in MeOH (based on a molecular weight of 482 g/mol for the seven main flavonolignan diastereoisomers). Then, 100 μL of this solution was dispensed into 0.7 mL miniature centrifuge tubes and allowed to dry overnight; this imparts 0.482 mg of silymarin per tube. The dried aliquots were stored at −20°C. For each experiment, aliquots of silymarin prepared as described above and in[64] were reconstituted in 40 μL of DMSO and extensively vortexed to generate a 25 mM stock solution. For all experiments, freshly prepared silymarin stock solutions were used once and then discarded. DMSO solvent controls were used for all experiments; for the microarray study the maximum DMSO concentration was 0.32%, while for some short duration signaling studies, when higher doses of silymarin were tested, the maximum DMSO concentration was 0.8–1.6%.

Microarray Design

Huh7.5.1 cells were plated at 75,000 cells/well were plated in 24-well plates, and the following day, media was replaced and incubated with 0.32% dimethylsulfoxide (DMSO) solvent control or silymarin at 83 μM (40 g/mL), a non-toxic dose.[63] Toxicity was monitored by ATPlite assay as described.[4] Each condition was performed in triplicate. Total

cellular RNA was isolated at four, eight, and 24 h post-silymarin exposure, with each triplicate condition being pooled. The study was performed on 4 separate technical replicates.

Microarray Analyses

Microarray data were background corrected, normalized and summarized using a robust multi-array average (RMA),[65] implemented in the Bioconductor oligo package.[66] Data were summarized at the transcript level. Comparisons at each time point were made by first fitting a weighted one-way analysis of variance (ANOVA) model,[67] and then computing empirical Bayes adjusted contrasts, using the Bioconductor limma package.[68] Transcripts were chosen with an unadjusted p-value < 0.05 and an absolute fold change > 1.5.

Various quality control plots were generated to ensure that both raw and summarized data fulfilled expectations. Density plots of the raw data indicated that the raw data were all distributed similarly, so a quantile normalization was warranted. False color images of each array showed no gross defects on the arrays, nor any entrapped bubbles. Plots of normalized unscaled standard errors (NUSE) from the RMA summarization step and relative log expression (RLE) plots were within expected ranges, and there were no outlier arrays on a principal components analysis (PCA) plot.

A weighted analysis of variance (ANOVA) model was used, which smoothly down-weights arrays that diverge from arrays with similar sample types. An unadjusted p-value < 0.05 and an absolute fold change > 1.5 was the selection criteria. These criteria were more conservative than using something more conventional such as a false discovery rate (FDR) of 5%. As an example, for the four-h contrast using a 5% FDR, there were 1882 significant genes. Using this criteria, only 308 genes were selected, thereby focusing on biologically significant genes by incorporating the additional fold change criterion.

Raw data (CEL files) and RMA summarized data have been submitted to the Gene Expression Omnibus (GEO) as GSE50994.

Validation of Microarray Results

Microarray results were confirmed by quantitative (Q)-RT-PCR using primer probe sets from Life Technologies shown in Table S1, Supporting Information. RNA was extracted with RNeasy extraction kit (Qiagen, Valencia, CA). Eighteen “Assay on Demand” gene expression assays (Applied Biosystems Inc., Hercules, CA) were run using the 96.96 Gene Expression Dynamic Array IFC (Fluidigm, South San Francisco, CA) according to the manufacturer’s instructions. All gene expression levels were measured in quintuplicate and normalized to beta-actin.

Bioinformatics Analyses, Protein Validation, and Signaling Studies

Ingenuity Pathway Analysis (IPA) software was used to predict and generate plausible regulatory networks (e.g. transcription factors or signaling kinases) to help explain changes observed in this study’s gene expression profile. Potential up- and down-regulators induced by silymarin-treatment were based on relationships in the molecular pathways (networks)

represented by published and experimentally observed gene expression, transcription events, and function annotation data, as well as the statistical likelihood of their association (i.e., p<value). To target regulators of interest, Z-scores were used to score and prioritize potential up- or down-regulators. Specifically, priority was given to Z-scores ≤ −2 and ≥ 2 of silymarin-induced gene expression data. The upstream regulator figures (a.k.a. “pinwheels”) were generated using IPA Path Designer (for legend see Figure S9, Supporting Information).

Based on IPA, protein induction/repression by silymarin was validated using Luminex kits (for CXCL10; Invitrogen) and western blots (for all other non-secreted proteins). Signaling studies assessed the level of phosphorylation of cellular proteins, using commercially available antibodies, and all blots shown in this study are representative of at least two independent experiments. Graphs of protein band pixel intensities were calculated by using J-Image. Band intensities were represented as fold-change of phosphorylated protein of total protein if total protein band intensity was available or, where specified, fold-change of the protein of interest of actin band intensity. The antibodies used are listed in Table S2, Supporting Information. Reporter gene assays were performed as described.[4] Reporter gene results were analyzed by one-tailed Student’s T-tests.

Metabolomics Analyses

For metabolomics studies, 1.5×10^6 Huh7TLR3 cells were plated in 60 mm dishes. After 2 d of cell growth, medium containing DMSO or 80 μM of silymarin was added to cells (n = 4, each). For harvesting, a quenching solution (60% methanol, 0.85% ammonium bicarbonate, stored at −80°C before use) was added to the dish for 1 min to quench metabolism. The quenching solution was then removed, 150 mM ammonium bicarbonate was added, and cells were scraped and moved into a 1.5 mL siliconized tube, which was then snap frozen in liquid nitrogen and stored at −80°C. Metabolites were extracted using chloroform/methanol (2:1 v/v) and chemically derivatized for analysis by gas chromatography-mass spectrometry (GC-MS), as previously described.[69–71] An Agilent 7890A gas chromatograph coupled with a single quadrupole 5975C mass spectrometer (Agilent Technologies, Santa Clara, CA) was used for metabolomics analyses, and metabolomics data were processed using MetaboliteDetector, as previously described.[69–72]

The integrated peak areas of identified metabolites were z-score transformed and visualized as a heat-map using InfernoRND (http://omics.pnl.gov/software/infernordn).[73,74]

The GC-MS data were $\log_{10}$ transformed and processed similarly to remove metabolites with inadequate information for statistical analyses and identify outlier GC-MS analyses. Metabolites were removed if they did not meet the minimum requirements for a t-test.[75] However, the data processing of the GC-MS raw files did not return any metabolites with inadequate data for statistics in either control or silymarin-treated cells at any time point. Extreme behavior in GC-MS datasets (outliers) was identified using a combination of correlation, principal component analysis (PCA), and an approach based on a robust Mahalanobis distance (rMd) to assess the reproducibility of the distribution of metabolite abundance values across biological replicates.[76] Strategies for normalization of the identified metabolite and unidentified metabolite feature abundances in each data matrix were evaluated using the Statistical Procedure for the Analyses of Normalization Strategies

(SPANS) protocol.[77] In particular, a Rank Invariant set as defined by a non-parametric test at a threshold of 0.05 was utilized to derive median values, and the data was subsequently median centered. Comparisons across time were performed by Analysis of Variance (ANOVA) with a Dunnett test correction to determine significance of each time point from the 1 h time point. Comparisons between DMSO and silymarin at a given time point were compared with a standard two-sample t-test.

Supplementary Material

Refer to Web version on PubMed Central for supplementary material.

Acknowledgments

We thank Amanda Milstein and Abigail Payne for technical assistance, Tyler Graf for preparation of single use silymarin aliquots, Benoit Viollet for AMPK wild type and knock out cells, and Leif W. Ellisen for DDIT4 wild type and knock out MEFs. We thank Nadja Cech and Edward Calabrese for insightful discussions.

Funding Sources

This work was supported by NIH grant 5R01AT006842 and 3R01AT006842-03S1 from NCCIH (formerly NCCAM), and the NIH Common Fund's Metabolomics Program, respectively. Support was also provided by the National Institute Of Environmental Health Sciences of the National Institutes of Health under Award Number P30ES007033. Metabolite measurements were performed in the Environmental Molecular Sciences Laboratory, a national scientific user facility sponsored by the U.S. Department of Energy (DOE) Office of Biological and Environmental Research and located at Pacific Northwest National Laboratory (PNNL). PNNL is a multi-program national laboratory operated by Battelle for the DOE under Contract DE-AC05-76RLO 1830.

ABBREVIATIONS

AMPK	adenosine monophosphate kinase
ATF4	activating transcription factor 4
DDIT4	DNA-damage-inducible transcript 4
EGCG	epigallocatechin gallate
ER	endoplasmic reticulum
FOXO	forkhead box O
KO	knock out
mTOR	mammalian target of rapamycin
MEF	murine embryo fibroblast
NF-κB	nuclear factor-kappa B
WT	wild type

References

1. Barnes PM, Bloom B, Nahin RL. National health statistics reports. 2008:1–23. [PubMed: 19361005]
2. Polyak SJ, Ferenci P, Pawlotsky JM. Hepatology. 2013; 57:1262–71. [PubMed: 23213025]
3. Ramasamy K, Agarwal R. Cancer Lett. 2008; 269:352–62. [PubMed: 18472213]

4. Polyak SJ, Morishima C, Lohmann V, Pal S, Lee DY, Liu Y, Graf TN, Oberlies NH. Proc Natl Acad Sci U S A. 2010; 107:5995–9. [PubMed: 20231449]
5. Deep G, Agarwal R. Cancer metastasis reviews. 2010; 29:447–63. [PubMed: 20714788]
6. Soria EA, Eynard AR, Bongiovanni GA. Basic & clinical pharmacology & toxicology. 2010; 107:982–7. [PubMed: 20735377]
7. Sanli T, Steinberg GR, Singh G, Tsakiridis T. Cancer Biol Ther. 2014; 15:156–69. [PubMed: 24100703]
8. Dizdaroglu M. Cancer Lett. 2012; 327:26–47. [PubMed: 22293091]
9. Gorrini C, Harris IS, Mak TW. Nature reviews Drug discovery. 2013; 12:931–47. [PubMed: 24287781]
10. Dibble CC, Manning BD. Nature cell biology. 2013; 15:555–64. [PubMed: 23728461]
11. Jewell JL, Guan KL. Trends Biochem Sci. 2013; 38:233–42. [PubMed: 23465396]
12. Nicklin P, Bergman P, Zhang B, Triantafellow E, Wang H, Nyfeler B, Yang H, Hild M, Kung C, Wilson C, Myer VE, MacKeigan JP, Porter JA, Wang YK, Cantley LC, Finan PM, Murphy LO. Cell. 2009; 136:521–34. [PubMed: 19203585]
13. Shaw RJ. Acta physiologica. 2009; 196:65–80. [PubMed: 19245654]
14. McGhee NK, Jefferson LS, Kimball SR. The Journal of nutrition. 2009; 139:828–34. [PubMed: 19297425]
15. Sofer A, Lei K, Johannessen CM, Ellisen LW. Mol Cell Biol. 2005; 25:5834–45. [PubMed: 15988001]
16. Hou J, Chong ZZ, Shang YC, Maiese K. Mol Cell Endocrinol. 2010; 321:194–206. [PubMed: 20211690]
17. Morishima C, Shuhart MC, Wang CC, Paschal DM, Apodaca MC, Liu Y, Sloan DD, Graf TN, Oberlies NH, Lee DY, Jerome KR, Polyak SJ. Gastroenterology. 2010; 138:671–81. 681 e1–2. [PubMed: 19782083]
18. Kolb H, Eizirik DL. Nature reviews Endocrinology. 2012; 8:183–92.
19. Piperi C, Adamopoulos C, Dalagiorgou G, Diamanti-Kandarakis E, Papavassiliou AG. J Clin Endocrinol Metab. 2012; 97:2231–42. [PubMed: 22508704]
20. Brownell J, Wagoner J, Lovelace ES, Thirstrup D, Mohar I, Smith W, Giugliano S, Li K, Crispe IN, Rosen HR, Polyak SJ. J Hepatol. 2013; 59:701–8. [PubMed: 23770038]
21. Sumpter R Jr, Loo YM, Foy E, Li K, Yoneyama M, Fujita T, Lemon SM, Gale M Jr. J Virol. 2005; 79:2689–99. [PubMed: 15708988]
22. Li K, Foy E, Ferreon JC, Nakamura M, Ferreon AC, Ikeda M, Ray SC, Gale M Jr, Lemon SM. Proc Natl Acad Sci U S A. 2005; 102:2992–7. [PubMed: 15710891]
23. Carter ME, Brunet A. Current biology : CB. 2007; 17:R113–4. [PubMed: 17307039]
24. Ellisen LW, Ramsayer KD, Johannessen CM, Yang A, Beppu H, Minda K, Oliner JD, McKeon F, Haber DA. Mol Cell. 2002; 10:995–1005. [PubMed: 12453409]
25. Horak P, Crawford AR, Vadysirisack DD, Nash ZM, DeYoung MP, Sgroi D, Ellisen LW. Proc Natl Acad Sci U S A. 2010; 107:4675–80. [PubMed: 20176937]
26. Schwarzer R, Tondera D, Arnold W, Giese K, Klippel A, Kaufmann J. Oncogene. 2005; 24:1138–49. [PubMed: 15592522]
27. Gingras AC, Gygi SP, Raught B, Polakiewicz RD, Abraham RT, Hoekstra MF, Aebersold R, Sonenberg N. Genes Dev. 1999; 13:1422–37. [PubMed: 10364159]
28. Laderoute KR, Amin K, Calaoagan JM, Knapp M, Le T, Orduna J, Foretz M, Viollet B. Mol Cell Biol. 2006; 26:5336–47. [PubMed: 16809770]
29. Hattori Y, Suzuki K, Hattori S, Kasai K. Hypertension. 2006; 47:1183–8. [PubMed: 16636195]
30. Lin CJ, Sukarieh R, Pelletier J. Mol Cancer Ther. 2009; 8:1606–12. [PubMed: 19509268]
31. Yang K, Chi H. Immunity. 2015; 42:4–6. [PubMed: 25607450]
32. Decleves AE, Mathew AV, Cunard R, Sharma K. Journal of the American Society of Nephrology : JASN. 2011; 22:1846–55. [PubMed: 21921143]
33. Ji G, Zhang Y, Yang Q, Cheng S, Hao J, Zhao X, Jiang Z. PLoS One. 2012; 7:e53101. [PubMed: 23300870]

34. Lamming DW, Ye L, Sabatini DM, Baur JA. J Clin Invest. 2013; 123:980–9. [PubMed: 23454761]
35. Roca H, Varsos ZS, Pienta KJ. Neoplasia. 2009; 11:1309–17. [PubMed: 20019839]
36. Steinberg GR, Kemp BE. Physiological reviews. 2009; 89:1025–78. [PubMed: 19584320]
37. Nakae J, Oki M, Cao Y. FEBS Lett. 2008; 582:54–67. [PubMed: 18022395]
38. Gharagozloo M, Javid EN, Rezaei A, Mousavizadeh K. Basic & clinical pharmacology & toxicology. 2013; 112:251–6. [PubMed: 23121838]
39. Dhanalakshmi S, Singh RP, Agarwal C, Agarwal R. Oncogene. 2002; 21:1759–67. [PubMed: 11896607]
40. Raina K, Agarwal C, Agarwal R. Mol Carcinog. 2013; 52:195–206. [PubMed: 22086675]
41. Singh RP, Agarwal R. Mol Carcinog. 2006; 45:436–42. [PubMed: 16637061]
42. Ben Sahra I, Regazzetti C, Robert G, Laurent K, Le Marchand-Brustel Y, Auberger P, Tanti JF, Giorgetti-Peraldi S, Bost F. Cancer Res. 2011; 71:4366–72. [PubMed: 21540236]
43. O'Neill LA, Hardie DG. Nature. 2013; 493:346–55. [PubMed: 23325217]
44. Scolletta S, Colletti M, Di Luigi L, Crescioli C. Mediators of inflammation. 2013; 2013:876319. [PubMed: 23690671]
45. Brownell J, Bruckner J, Wagoner J, Thomas E, Loo YM, Gale M Jr, Liang TJ, Polyak SJ. J Virol. 2014; 88:1582–90. [PubMed: 24257594]
46. Brownell J, Polyak SJ. Clin Cancer Res. 2013; 19:1347–52. [PubMed: 23322900]
47. Jiao Y, Zhang T, Wang R, Zhang H, Huang X, Yin J, Zhang L, Xu X, Wu H. Viral immunology. 2012; 25:333–7. [PubMed: 22788418]
48. Inoki K, Zhu T, Guan KL. Cell. 2003; 115:577–90. [PubMed: 14651849]
49. Liu M, Wilk SA, Wang A, Zhou L, Wang RH, Ogawa W, Deng C, Dong LQ, Liu F. J Biol Chem. 2010; 285:36387–94. [PubMed: 20851890]
50. Shirakami Y, Shimizu M, Moriwaki H. Curr Drug Targets. 2012; 13:1842–57. [PubMed: 23140294]
51. Shor B, Gibbons JJ, Abraham RT, Yu K. Cell Cycle. 2009; 8:3831–7. [PubMed: 19901542]
52. Wu D, Wang J, Pae M, Meydani SN. Molecular aspects of medicine. 2012; 33:107–18. [PubMed: 22020144]
53. Shishodia S. BioFactors. 2013; 39:37–55. [PubMed: 22996381]
54. Zhang Q, Kelly AP, Wang L, French SW, Tang X, Duong HS, Messadi DV, Le AD. The Journal of investigative dermatology. 2006; 126:2607–13. [PubMed: 16841034]
55. Hardie DG, Ross FA, Hawley SA. Chem Biol. 2012; 19:1222–36. [PubMed: 23102217]
56. Kostyuk VA, Potapovich AI, Suhan TO, de Luca C, Korkina LG. European journal of pharmacology. 2011; 658:248–56. [PubMed: 21371465]
57. Belguise K, Guo S, Sonenshein GE. Cancer Res. 2007; 67:5763–70. [PubMed: 17575143]
58. Dudekula N, Arora V, Callaerts-Vegh Z, Bond RA. Dose-response : a publication of International Hormesis Society. 2005; 3:414–24. [PubMed: 18648614]
59. Calabrese EJ, Blain RB. Regulatory toxicology and pharmacology : RTP. 2011; 61:73–81. [PubMed: 21699952]
60. Calabrese V, Cornelius C, Dinkova-Kostova AT, Iavicoli I, Di Paola R, Koverech A, Cuzzocrea S, Rizzarelli E, Calabrese EJ. Biochim Biophys Acta. 2012; 1822:753–83. [PubMed: 22108204]
61. Zhong J, Gastaminza P, Cheng G, Kapadia S, Kato T, Burton DR, Wieland SF, Uprichard SL, Wakita T, Chisari FV. Proc Natl Acad Sci U S A. 2005; 102:9294–9. [PubMed: 15939869]
62. Li K, Chen Z, Kato N, Gale M Jr, Lemon SM. J Biol Chem. 2005; 280:16739–47. [PubMed: 15737993]
63. Wagoner J, Negash A, Kane OJ, Martinez LE, Nahmias Y, Bourne N, Owen DM, Grove J, Brimacombe C, McKeating JA, Pecheur EI, Graf TN, Oberlies NH, Lohmann V, Cao F, Tavis JE, Polyak SJ. Hepatology. 2010; 51:1912–21. [PubMed: 20512985]
64. Graf TN, Wani MC, Agarwal R, Kroll DJ, Oberlies NH. Planta Med. 2007; 73:1495–501. [PubMed: 17948171]
65. Irizarry RA, Hobbs B, Collin F, Beazer-Barclay YD, Antonellis KJ, Scherf U, Speed TP. Biostatistics. 2003; 4:249–64. [PubMed: 12925520]

66. Carvalho BS, Irizarry RA. Bioinformatics. 2010; 26:2363–7. [PubMed: 20688976]
67. Ritchie ME, Diyagama D, Neilson J, van Laar R, Dobrovic A, Holloway A, Smyth GK. BMC Bioinformatics. 2006; 7:261. [PubMed: 16712727]
68. Smyth GK, Michaud J, Scott HS. Bioinformatics. 2005; 21:2067–75. [PubMed: 15657102]
69. Kim YM, Schmidt BJ, Kidwai AS, Jones MB, Deatherage Kaiser BL, Brewer HM, Mitchell HD, Palsson BO, McDermott JE, Heffron F, Smith RD, Peterson SN, Ansong C, Hyduke DR, Metz TO, Adkins JN. Molecular bioSystems. 2013; 9:1522–34. [PubMed: 23559334]
70. Deatherage Kaiser BL, Li J, Sanford JA, Kim YM, Kronewitter SR, Jones MB, Peterson CT, Peterson SN, Frank BC, Purvine SO, Brown JN, Metz TO, Smith RD, Heffron F, Adkins JN. PLoS One. 2013; 8:e67155. [PubMed: 23840608]
71. Cole JK, Hutchison JR, Renslow RS, Kim YM, Chrisler WB, Engelmann HE, Dohnalkova AC, Hu D, Metz TO, Fredrickson JK, Lindemann SR. Frontiers in microbiology. 2014; 5:109. [PubMed: 24778628]
72. Webb-Robertson BJ, Kim YM, Zink EM, Hallaian KA, Zhang Q, Madupu R, Waters KM, Metz TO. Metabolomics : Official journal of the Metabolomic Society. 2014; 10:897–908. [PubMed: 25254001]
73. Polpitiya AD, Qian WJ, Jaitly N, Petyuk VA, Adkins JN, Camp DG 2nd, Anderson GA, Smith RD. Bioinformatics. 2008; 24:1556–8. [PubMed: 18453552]
74. Taverner T, Karpievitch YV, Polpitiya AD, Brown JN, Dabney AR, Anderson GA, Smith RD. Bioinformatics. 2012; 28:2404–6. [PubMed: 22815360]
75. Webb-Robertson BJ, McCue LA, Waters KM, Matzke MM, Jacobs JM, Metz TO, Varnum SM, Pounds JG. J Proteome Res. 2010; 9:5748–56. [PubMed: 20831241]
76. Matzke MM, Waters KM, Metz TO, Jacobs JM, Sims AC, Baric RS, Pounds JG, Webb-Robertson BJ. Bioinformatics. 2011; 27:2866–72. [PubMed: 21852304]
77. Webb-Robertson BJ, Matzke MM, Jacobs JM, Pounds JG, Waters KM. Proteomics. 2011; 11:4736–41. [PubMed: 22038874]

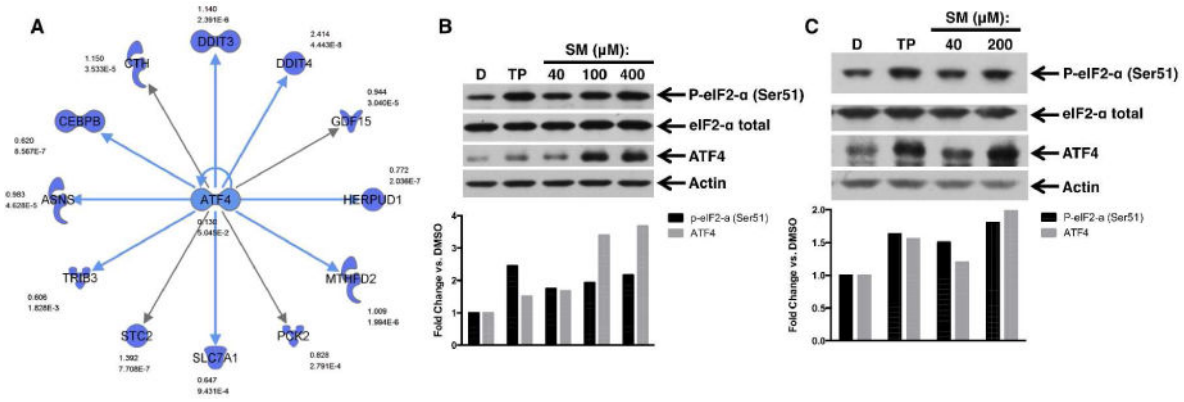

Figure 1.

Silymarin induces ER stress. A, ATF4-regulated genes (as shown on the outside of these pinwheels with the log-fold [top] and p-value [bottom] data located next to each gene) were all up-regulated (blue) in Huh7.5.1 cells at four h post-silymarin treatment. B, Huh7.5.1 cells were treated with DMSO (D) thapsigarin (TP; 100 nM), and the indicated μM doses of silymarin (SM) for one h prior to whole cell protein extraction. Whole cell lysates were analyzed by Western blot and probed for ER stress targets: P-eIF2-α(Ser51), eIF2-α total, and ATF4, as well as Actin (loading control). C, Jurkat cells were treated as described above, harvested at one-h post silymarin-treatment, and the expression of ER stress targets were analyzed. Below panels B and C are fold-change of protein band pixel intensity between D versus TP or silymarin treatments.

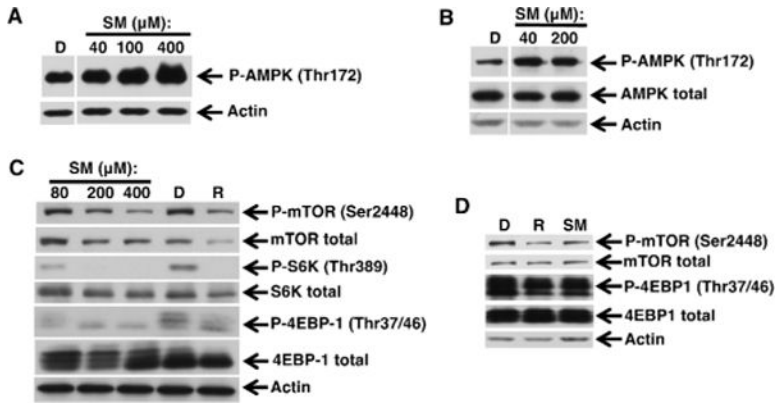

Figure 2.

Silymarin treatment activates AMPK and inhibits mTOR signaling. Huh7.5.1 (panel A) and Jurkat cells (panel B) were treated with DMSO (D) or the indicated doses of silymarin (μM) for one-h followed by whole cell protein extraction and Western blotting for AMPK activation (i.e. phosphorylation on Thr172) and Actin targets. Panel C, Huh7.5.1 cells were serum-starved overnight, then treated with DMSO (D), rapamycin (R; 10 nM), or the indicated micromolar (μM) doses of silymarin (SM) for one h, before cells were serum-activated with FBS (10% final) for 10 minutes. Whole cell protein extracts were harvested, analyzed by Western blot, and probed for mTOR substrate targets: P-mTOR, mTOR total, P-S6K, S6K total, P-4EBP-1, and 4EBP1 total, as well as Actin. Panel D, Jurkat cells were cultured in complete medium followed by treatment with D, R, or 80 μM silymarin (SM) for two h prior to protein harvest.

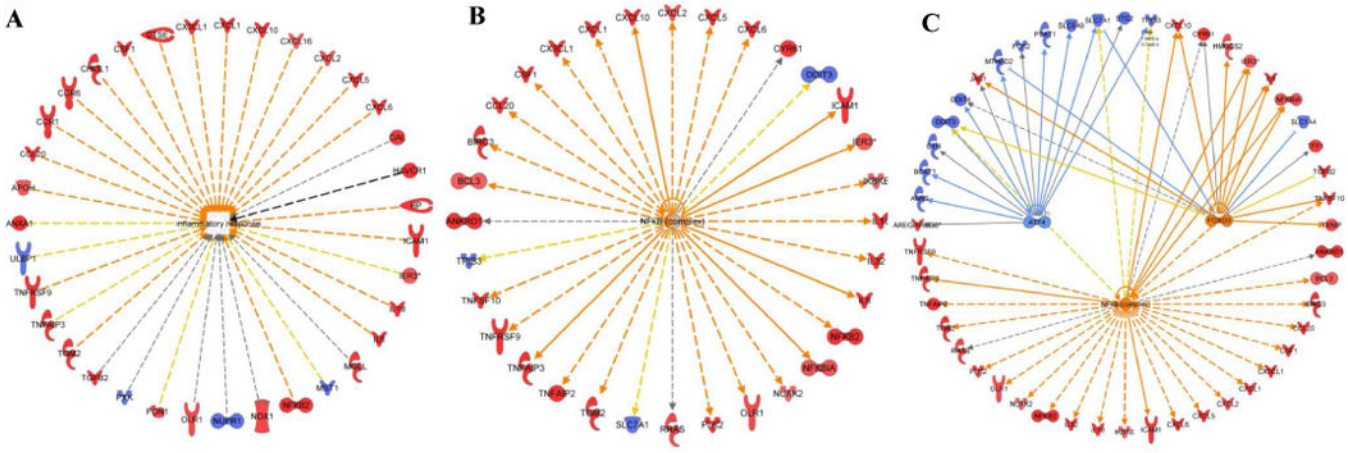

Figure 3.

Silymarin suppresses inflammatory signaling. A, IPA predicted silymarin treatment to be involved in the inflammatory response based on the down-regulation of many inflammatory-related genes. B, Silymarin treatment results in the significant down-regulation of NF-κB-related genes. C, Many of the genes significantly regulated with silymarin treatment in Huh7.5.1 cells by 24 h are shared between the ATF4, FOXO3, and NF-κB pathways.

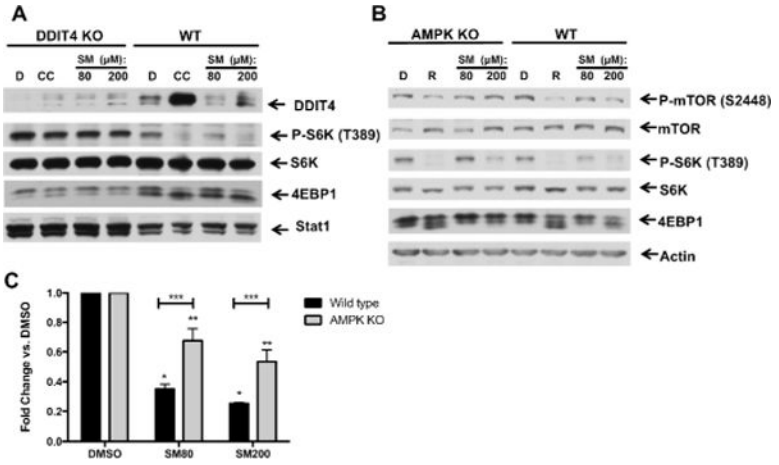

Figure 4.

Silymarin inhibits mTOR in part via DDIT4 and AMPK, and silymarin inhibits NF-κB in part via AMPK. A, Silymarin suppression of mTOR is partially dependent on DDIT4. Wild type (WT) and DDIT4 knockout (DDIT4 KO) MEFs were treated with DMSO (D), cobalt chloride (CC, 200 μM) or silymarin (SM) at 80 or 200 μM; labeled as 80 and 200 in the figure. Cell lysates were harvested at four h and probed for DDIT4 and the indicated mTOR proteins. B, Silymarin suppression of mTOR is partially AMPK dependent. WT or AMPK KO MEFs were treated with DMSO (D), 10nM rapamycin (R), or silymarin at 80 or 200 μM. Cell lysates were harvested at four h and probed for the indicated mTOR proteins. C, Silymarin suppression of NF-κB activation is partially dependent on AMPK. WT or AMPK KO MEFs were transfected with pRDII-luc, a plasmid that express luciferase under control of the NF-κB site from the IFN-β promoter. Twenty h later, cells were treated with silymarin (80 or 200 μM) or D for one h prior to stimulation with 100 ηg/mL TNF-α for three h. The data shown represent the mean averages and standard deviations of four independent technical repeats. Single asterisk (*) denotes p values of < 0.02 from one-sided T tests of silymarin-treated samples relative to D control for AMPK WT MEFs. Double asterisk (**) denotes p values of < 0.02 from one-sided T tests of silymarin-treated samples relative to D control for AMPK KO MEFs. Triple asterisk (***) denotes p values of < 0.02 from one-sided T tests of silymarin treated WT vs. AMPK KO MEFs.

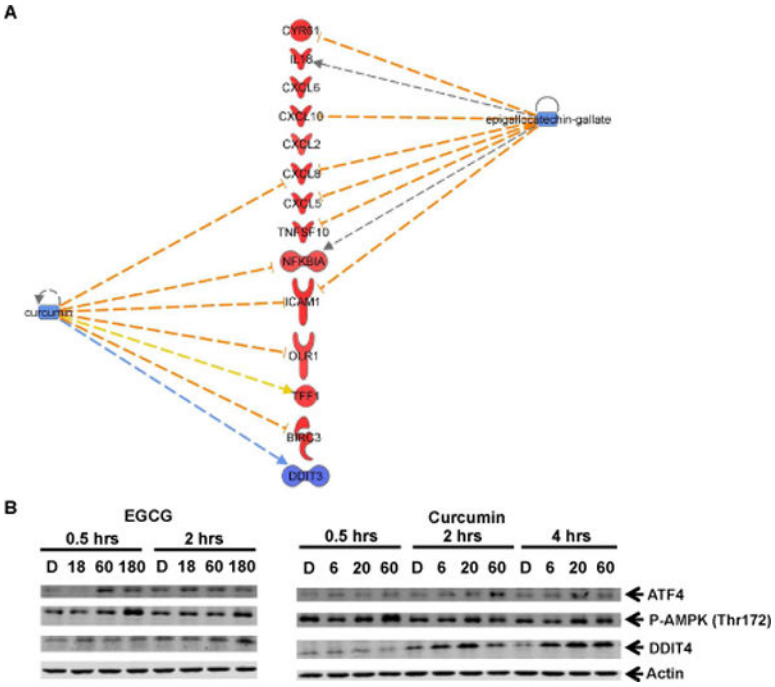

Figure 5.

Chemically distinct natural products engage similar stress responses. A, IPA predicted that other natural products, such as EGCG and curcumin, induce similar gene expression changes in comparison to silymarin treatment in Huh7.5.1 cells at 24 h post-silymarin treatment. B, Huh7.5.1 cells were treated with EGCG, curcumin, or DMSO (D) solvent control for 0.5, two, or four h and whole cell protein lysates were analyzed by Western blotting with the indicated antibodies. The μM doses of each compound are EGCG: 18, 60, and 180, and Curcumin: six, 20, and 60.

Table 1

Effect of Silymarin on the Metabolome of Huh7TLR3 Cells.

	t-test P-value			fold change (SM/DMSO)		
metabolites	**4h**	**8h**	**24h**	**4h**	**8h**	**24h**
glycolytic intermediates						
D-glucose	0.691	0.191	0.004	−1.060	−1.194	−1.451
D-glucose-6-phosphate	0.082	0.183	0.005	−1.993	−1.412	−3.321
glycerol 3-phosphate	0.003	0.001	0.000	−1.975	−1.748	−2.065
dihydroxyacetone phosphate	0.001	0.010	0.197	−1.546	−1.274	−1.095
DL-glyceraldehyde 3-phosphate	0.060	0.461	0.017	−2.225	−1.208	−1.783
3-phosphoglycerate	0.070	0.080	0.241	−1.414	−1.317	−1.558
pyruvic acid	0.895	0.000	0.020	1.030	−1.630	−1.835
TCA cycle intermediates						
citric acid	0.030	0.004	0.000	−1.620	−1.808	−2.859
alpha-ketoglutaric acid	0.003	0.018	0.001	−1.973	−2.175	−4.110
alpha-hydroxyglutaric acid (NIST)	0.159	0.048	0.437	−1.267	−1.465	1.625
succinic acid	0.003	0.001	0.000	−1.573	−1.999	−2.813
fumaric acid	0.185	0.464	0.443	1.281	−1.193	−1.322
D-malic acid	0.193	0.018	0.001	−1.188	−1.307	−1.693
amino acids and intermediates						
alpha-aminoadipic acid (NIST)	0.536	0.006	0.360	−1.172	−1.916	−1.260
L-alanine	0.396	0.114	0.116	−1.158	−1.289	−1.231
L-aspartic acid	0.020	0.019	0.075	−1.482	−1.542	−1.264
L-cysteine	0.067	0.197	0.180	1.403	1.399	1.514
L-glutamic acid	0.022	0.108	0.027	−1.467	−1.434	−1.390
glutamine	0.146	0.174	0.111	−1.233	−1.234	−1.306
glycine	0.646	0.664	0.037	1.054	−1.044	1.301
DL-isoleucine	0.405	0.358	0.438	1.116	−1.100	−1.070
L-phenylalanine	0.925	0.824	0.898	−1.014	1.014	1.012
L-pyroglutamic acid	0.115	0.013	0.003	−1.287	−1.332	−1.446
L-serine	0.051	0.001	0.003	−1.474	−1.674	−1.708
L-threonine	0.166	0.022	0.039	−1.242	−1.289	−1.292

	t-test P-value			fold change (SM/DMSO)		
metabolites	**4h**	**8h**	**24h**	**4h**	**8h**	**24h**
L-tyrosine	0.088	0.353	0.041	1.666	1.311	1.471
L-valine	0.809	0.237	0.165	1.037	−1.210	−1.170
urea cycle and intermediates						
4-guanidinobutyric acid	0.053	0.313	0.214	−1.386	−1.180	1.117
urea	0.827	0.742	0.026	−1.088	−1.090	−2.106
non-proteogenic amino acids and related compounds						
N-acetyl-L-aspartic acid	0.151	0.380	0.016	−1.264	−1.116	−1.528
aminomalonic acid (NIST)	0.046	0.222	0.420	−2.249	−1.381	−1.374
creatinine	0.100	0.038	0.002	−4.872	−2.066	−2.853
dehydroalanine (possibly from cysteine)	0.040	0.044	0.218	1.179	−1.272	−1.177
nucleobases, nucleosides, and intermediates						
adenine	0.765	0.700	0.110	−1.071	1.097	−1.834
adenosine	0.983	0.078	0.334	1.010	1.500	2.151
D-ribose-5-phosphate	0.199	0.685	0.498	−1.235	−1.063	−1.168
thymine	0.546	0.842	0.118	−1.175	−1.041	−1.503
uracil	0.779	0.470	0.262	−1.107	1.387	−1.808
B vitamins and intermediates						
beta-alanine	0.057	0.265	0.010	−1.941	−1.294	−1.345
pantothenic acid	0.001	0.000	0.000	2.559	2.603	2.237
porphine	0.700	0.607	0.101	1.155	1.137	−1.943
ribitol	0.993	0.111	0.095	1.001	−1.508	−1.350
sugars, sugar acids, and sugar alcohols						
fructose	0.588	0.031	0.006	−1.075	−1.292	−1.710
gluconic acid	0.151	0.003	0.009	−3.579	−2.115	−2.102
D-mannitol	0.307	0.005	0.006	−1.200	−1.466	−1.764
Inositols and intermediates						
inositol phosphate (NIST)	0.242	0.352	0.030	−1.246	−1.126	−1.506
myo-inositol	0.057	0.031	0.011	−1.348	−1.302	−1.600
free fatty acids						
oleic acid	0.339	0.164	0.431	1.191	1.255	1.142

J Nat Prod. Author manuscript; available in PMC 2016 August 28.

	t-test P-value			fold change (SM/DMSO)		
metabolites	**4h**	**8h**	**24h**	**4h**	**8h**	**24h**
stearic acid	0.252	0.963	0.085	1.135	1.005	−1.254
miscellaneous molecules						
carbonate ion	0.308	0.738	0.171	−1.439	−1.078	−1.509
l-(+) lactic acid	0.846	0.763	0.014	1.027	−1.035	−1.386
2-ketoisocaproic acid	0.156	0.235	0.048	1.293	−1.104	−1.426
phosphoric acid	0.937	0.784	0.143	1.010	−1.039	−1.166
methylphosphate (NIST)	0.472	0.702	0.154	1.122	−1.045	−1.213

[a] Fold change in metabolite concentrations in SM (80 μM) versus DMSO treatments over four, eight, and 24 h.

[b] The experiment was performed on quadruplicate technical replicates.